Proceedings of the 4th International Conference on Functional Materials and Civil Engineering
DOI: 10.54254/2755-2721/2026.37436

Rethinking Powerline Energy Harvesting: From Induced Voltage to Usable Power

Ziyang Cai

Department of Electrical and Electronic Engineering, University of Nottingham Ningbo China, Ningbo, China
ssyzc11@gmail.com

Abstract. Powerline magnetic energy harvesting offers a non-invasive route to supply low-power monitoring nodes, but a substantial induced voltage does not necessarily imply that usable electrical power can be delivered through the power-conversion interface. This paper investigates that voltage-to-power gap using a ferrite-core inductive harvester. The front end was designed for an induced voltage of approximately 6 V and produced 5.33 V AC under a controlled 10 A, 50 Hz line condition. Despite this measured voltage, the bridge-rectifier output was 0 V DC, preventing the real harvesting chain from establishing usable downstream energy. A simplified source-impedance simulation qualitatively reproduces the progression from stable rectification for an ideal source to severe voltage collapse when source impedance and load are introduced. The results support a system-level interpretation in which source impedance, rectification loss, and interface loading jointly constrain energy delivery. Powerline harvesters should therefore be evaluated around loaded power delivery rather than induced voltage alone.

Keywords: Powerline energy harvesting, Electromagnetic induction, Source impedance, Rectification, Low-power sensing

1. Introduction

Powerline condition monitoring increasingly relies on distributed low-power sensing to observe electrical and thermal states without frequent human intervention. Supplying these nodes is difficult when installation points are inaccessible or long maintenance intervals are required. Magnetic energy harvesting provides a non-invasive option because alternating line current produces a time-varying magnetic field that can be coupled through a magnetic core and pickup winding [1-4]. This makes current-transformer-based harvesting attractive for local sensor power without direct electrical contact with the conductor.

The presence of an induced voltage, however, is not equivalent to the delivery of usable power. A practical harvesting chain must convert the coil output through rectification and filtering, interface with a power-management integrated circuit (PMIC), accumulate energy in storage, and finally support a load. Under these conditions, winding resistance, source/load impedance mismatch, rectifier forward-voltage loss, and PMIC input behavior can substantially alter the voltage seen at

© 2026 The Authors. This is an open access article distributed under the terms of the Creative Commons Attribution License 4.0 (https://creativecommons.org/licenses/by/4.0/).

DOI: 10.54254/2755-2721/2026.37436

the source terminals [5-9]. A voltage measured under light loading can therefore overstate the energy available after the conversion interface is connected.

The prototype examined in this paper exposes this distinction directly. The electromagnetic front end was designed for approximately 6 V and produced 5.33 V AC at 10 A and 50 Hz, whereas the subsequent bridge-rectifier output was measured as 0 V DC. Consequently, the real harvesting chain did not establish downstream storage charging or regulated output. This observation motivates the central research question of this work: why can a powerline harvester exhibit a substantial induced voltage while failing to deliver usable power through a practical power-conversion interface?

The paper makes three contributions around this question. First, it experimentally characterizes a ferrite-core prototype that provides a controlled platform for examining the voltage-to-power gap rather than treating the coil itself as the main novelty. Second, it identifies the 5.33 V AC-to-0 V DC transition as the key system-level observation separating front-end induction from usable downstream energy. Third, it uses a simplified source-impedance simulation as mechanism-level support, showing that the experimentally observed collapse is consistent with the combined effects of source impedance, rectification loss, and loading. These findings motivate a power-delivery-centric approach to harvester design and evaluation.

2. Related work

Powerline magnetic energy harvesting has been investigated using current-transformer-like structures, toroidal and split magnetic cores, and winding or core optimization to increase extracted energy. Studies have addressed transmission-line harvesting [1-3], experimental characterization of inductive harvesters [4], manipulation of magnetic fields to improve current-transformer energy extraction [5], saturation-aware core design [6], analytical models for magnetic harvesters [7, 8], and stable-output structures based on magnetic-core behavior [10]. Practical demonstrations have also used powerline magnetic harvesters to support wireless-sensor applications [11, 12]. Experimental characterization work further shows that the apparent performance of an inductive harvester depends on the selected load, the magnetic operating point, and the conditioning circuit, so voltage and power metrics must be interpreted together [4]. Collectively, this literature establishes the feasibility of the magnetic harvesting front end and shows that induced voltage and harvested power depend strongly on core, winding, current, saturation, and load conditions. It also suggests that a front-end voltage value is most meaningful when it is accompanied by information about the electrical condition under which it was measured.

A second research line concerns the interface required to convert energy from a weak or high-impedance source. Powerline harvesting studies have used matching networks and specialized management circuits to improve power transfer [9], while passive and active rectifier analyses show that diode conduction loss and rectifier topology can materially affect usable output [13]. More generally, magnetic-harvester models emphasize that the load interacts with the source rather than receiving energy from an ideal voltage generator [7, 8]. Ultra-low-power PMICs such as the BQ25570 are designed to regulate the input of high-impedance energy sources and provide boost conversion, MPPT, and storage management [14], but their effectiveness still depends on adequate energy reaching the DC input node. This distinction is important because MPPT or input-voltage regulation cannot recover energy that has already been lost through source collapse or unsuccessful rectification. The conversion interface must therefore be considered jointly with the electromagnetic source rather than appended after the front-end design is complete.

These two research lines motivate a more explicit system-level evaluation question. Prior work demonstrates that magnetic induction from power conductors is feasible and that optimized systems

DOI: 10.54254/2755-2721/2026.37436

can deliver useful power, yet a relatively high measured front-end voltage does not by itself establish that the same source can sustain a real rectifier, PMIC, and storage interface. The present work therefore focuses on whether a substantial measured induced voltage remains representative of usable energy after practical interface loading is introduced. The 5.33 V AC-to-0 V DC observation provides a compact experimental case for examining this gap, while the source-impedance model is used only to support a plausible mechanism rather than to claim an exact measured cause.

3. From induced voltage to usable power

3.1. System architecture

Fig. 1 reduces the prototype to the energy path relevant to the research question. Alternating line current establishes magnetic flux in the ferrite core; the pickup winding generates an AC voltage V_{AC} (V); a bridge rectifier and filter attempt to form a DC voltage V_{DC} (V); the BQ25570 represents the downstream power-management interface; and a supercapacitor provides energy storage before a regulated load. Three observation points are therefore sufficient for the analysis: the induced AC voltage, the rectified DC voltage, and the storage/output state. The object of study is the coupled source-interface-storage chain, not the pickup coil in isolation.

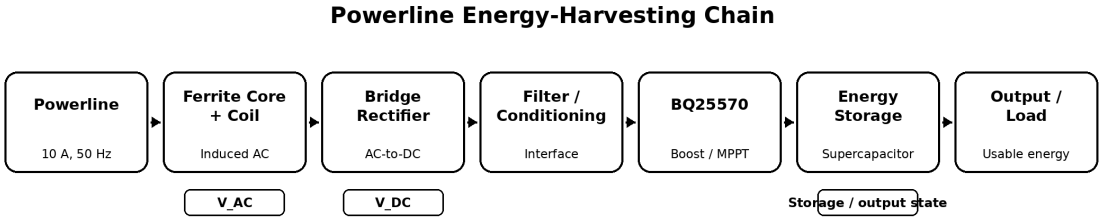

Figure 1. Simplified powerline energy-harvesting chain and the three key observation points used in this paper

3.2. Electromagnetic harvester design

For a sinusoidal flux, Faraday's law gives an induced RMS electromotive force $V_{ind,rms}$ (V) proportional to frequency f (Hz), winding turns N (dimensionless), and peak magnetic flux Φ_m (Wb). For the current-transformer-like geometry used here, Φ_m depends on the magnetic field established by the line current and the effective magnetic-core geometry. The peak magnetic flux density B_m is expressed in teslas (T), and the effective core cross-sectional area A_e is expressed in square metres (m²). The compact design relation is

$$V_{ind,rms} \approx 4.44\, f\, N\, \Phi_m, \qquad \Phi_m = B_m\, A_e. \tag{1}$$

The prototype was designed to generate several volts while remaining physically windable. The retained design parameters are approximately 400 turns, a 0.4 mm wire diameter, an effective core cross-sectional area of about 225 mm², and a magnetic path length of about 220 mm. The intended operating point was 10 A at 50 Hz, for which the analytical design target was approximately 6 V. Table 1 lists only the parameters required to connect the electromagnetic design to the experimental result.

DOI: 10.54254/2755-2721/2026.37436

Table 1. Key harvester design parameters

Parameter	Value
Core cross-sectional area	≈225 mm²
Magnetic path length	≈220 mm
Coil turns	≈400
Wire diameter	0.4 mm
Test frequency	50 Hz
Test line current	10 A
Analytical target voltage	≈6 V

3.3. Source loading and the voltage-to-power gap

The measured induced voltage does not directly specify how much power the source can deliver. As a first-order explanation, the pickup coil can be represented by a Thévenin-style open-circuit voltage V_{OC} (V) in series with a source resistance R_s (Ω). This representation is intentionally simplified: R_s was not directly measured in the thesis and is not treated here as an experimentally identified parameter. With a finite load resistance R_L (Ω), the terminal voltage V_L (V) is

$$V_L = V_{OC} \cdot R_L/(R_S + R_L). \quad (2)$$

A high-impedance meter can therefore measure a voltage near V_{OC} while an attached rectifier or converter produces a larger current-dependent drop across the source impedance. The bridge rectifier further reduces the limited voltage budget because two diode junctions conduct in each half-cycle. At low available current, this nonlinear interface can interact strongly with the source rather than behave as an ideal voltage follower. The mechanism considered in this paper comprises the following stages: (1) a high induced voltage is measured under light loading; (2) the connected interface loads the source; (3) the terminal voltage collapses; (4) rectification introduces further loss; (5) the DC input becomes insufficient; and (6) usable downstream energy cannot be established. Section 4 evaluates whether the experiment and the existing simulation are consistent with this sequence.

4. Experimental evaluation

4.1. Experimental setup

The experimental setup used a toroidal ferrite core with a wound pickup coil placed around a conductor carrying approximately 10 A AC at 50 Hz. The pickup was connected to the bridge rectifier/filter and then to the BQ25570 energy-management stage; a 100 F supercapacitor was connected as the storage element. Measurements were staged to separate front-end induction from downstream conversion: the coil AC voltage was recorded first, followed by the rectified DC node and the storage/output state. This staged structure is sufficient to determine where usable energy ceased to propagate through the chain without reproducing the equipment-procurement and wiring history of the prototype-development record. The measurement sequence also prevents a downstream result from being misinterpreted when its upstream input condition has not been

DOI: 10.54254/2755-2721/2026.37436

established. In particular, a PMIC or storage-stage test can only be treated as part of end-to-end harvesting if the electrical energy applied to that stage originates from the real magnetic-harvesting front end.

4.2. Induced-voltage validation

At the 10 A, 50 Hz test point, the pickup coil produced a measured induced voltage of 5.33 V AC compared with the approximately 6 V analytical design target. The relative difference is about 11.2%; this value is stated once as a comparison with the design target and is not a formal uncertainty or model-error bound. The remaining difference is plausibly associated with non-uniform magnetic field distribution, imperfect coupling and leakage flux, winding parasitics, current variation, and measurement uncertainty. These non-ideal effects are not expanded further because the central issue is not the small deviation from 6 V but the much larger change after interface connection.

Viewed only at the coil terminals, 5.33 V AC might suggest that the harvester front end is functioning adequately. The decisive next question is whether that voltage remains representative of usable energy after the power-conversion interface is attached. Fig. 2 presents the prototype and the measured voltage evidence without the prototype-development record captions, so the figure serves only as the experimental narrative of this paper.

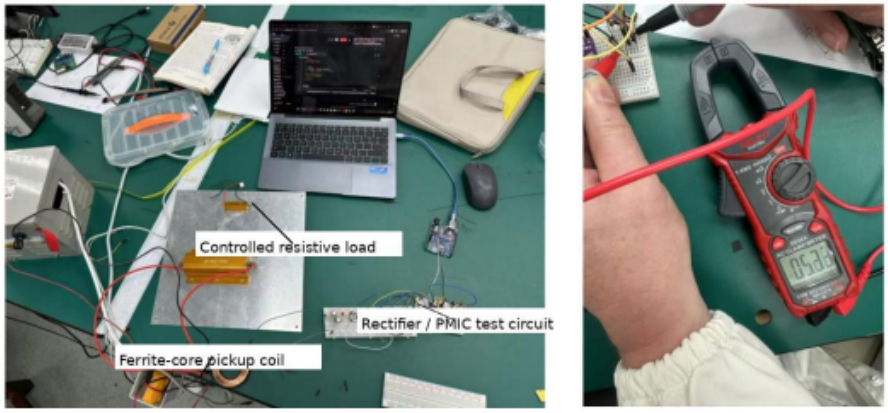

(a) Experimental prototype (b) Measured induced voltage

Figure 2. (a) Experimental prototype with key components identified and (b) measured induced voltage of 5.33 V AC at approximately 10 A and 50 Hz

4.3. Discrepancy between induced AC voltage and rectified DC output

Despite 5.33 V AC at the coil output, the rectifier output was measured as 0 V DC. This is the central experimental observation of the paper. With no valid rectified input from the real harvesting chain, the connected 100 F supercapacitor showed no observable charging and a regulated downstream output could not be established. The evidence therefore supports successful voltage induction at the magnetic front end, but it does not support end-to-end self-powered operation.

The key analytical distinction is between the physical coil and an ideal voltage source. An idealized 5.33 V source can sustain the rectifier in simulation because it has negligible internal impedance and unrestricted current for the modeled operating point. The physical coil has finite internal resistance and limited current capability; once the rectifier and subsequent circuit load the source, terminal voltage can fall while the conducting diode pair consumes additional voltage

DOI: 10.54254/2755-2721/2026.37436

headroom. Component and wiring checks were part of the original development process, but they are not treated here as the research narrative. Instead, the source-loading interpretation is presented as a mechanism-consistent explanation that is tested qualitatively against the existing simulation. This wording is deliberately narrower than claiming a uniquely identified root cause: the available measurements establish the voltage collapse across the chain, while the model shows that finite source impedance and load interaction are capable of producing the same qualitative behavior.

4.4. Source-impedance simulation

The existing simulation model considered three qualitative cases. Case 1 used an ideal source with no source impedance and produced a stable rectified response. Case 2 introduced source impedance and showed a clear reduction in the output envelope. Case 3 combined source impedance with loading and produced a progression toward near-zero output. Fig. 3 reproduces these three cases with a unified paper caption. The simulation is used as qualitative mechanism support: it reproduces the direction of the observed collapse and is consistent with the hypothesis that source/interface interaction can prevent a substantial lightly loaded voltage from producing useful downstream DC. The useful comparison is therefore the progression across the three cases rather than the absolute simulated voltage values. Case 1 establishes the behavior expected when the source can maintain its terminal voltage; Case 2 shows the penalty introduced by source impedance; and Case 3 shows how additional loading can move the operating point toward negligible output.

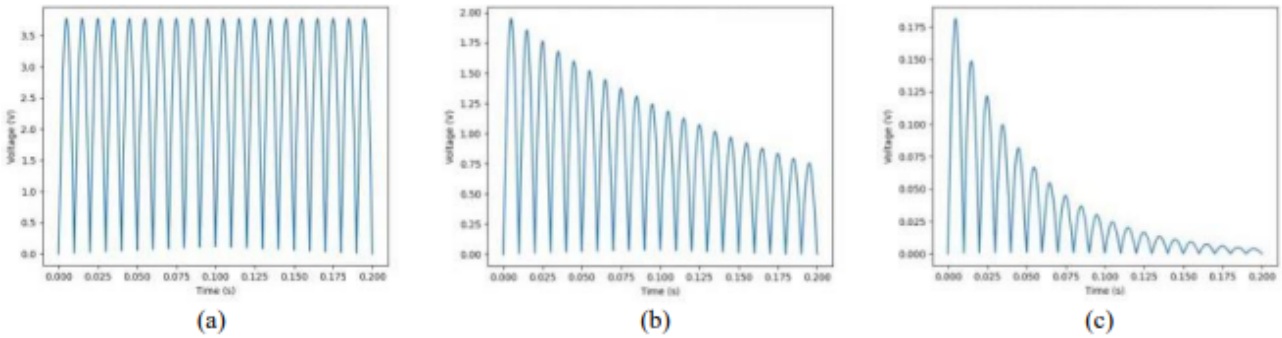

Figure 3. Illustrative qualitative source-impedance simulation: (a) ideal source, (b) source impedance, and (c) source impedance with load, showing progressive voltage collapse

The model does not identify the actual source resistance of the prototype and does not constitute quantitative validation of the failure mechanism. The coil is represented by an ideal source plus lumped resistance, while distributed parasitics, nonlinear magnetic behavior, and a full switching model of the BQ25570 are not included. Accordingly, the appropriate interpretation is that the simulation supports a plausible mechanism and qualitatively reproduces the trend; it does not prove an exact cause, predict harvested power, or establish conversion efficiency.

4.5. Stage-level findings and isolated BQ25570 test

The downstream BQ25570 was also exercised independently using two 1.5 V cells in series, providing approximately 3 V DC in place of the rectifier output. This isolation test separates downstream module testability from the real harvesting-chain result. It shows that the BQ25570 stage could be tested under an external stable source; it does not show that the powerline harvester

DOI: 10.54254/2755-2721/2026.37436

successfully supplied that stage. Table 2 summarizes the evidence without extending the claims beyond the measured observations.

Table 2. Stage-level experimental findings

Stage	Input / condition	Observed result	Interpretation
Magnetic harvesting	10 A, 50 Hz	5.33 V AC	Front-end voltage induction observed
Rectification	Real coil input	0 V DC	No usable rectified DC observed
Storage	Real harvesting chain	No observable charging	No usable upstream energy reached storage
BQ25570 isolation	External ≈3 V DC	Module tested independently	Downstream test only; not end-to-end harvesting

5. Discussion

First, voltage alone is an insufficient evaluation metric for a weak energy source. The contrast between 5.33 V AC at the coil and 0 V DC after rectification shows why a front-end voltage measurement cannot be equated with deliverable power. A stronger evaluation should include loaded terminal behavior, rectified output, storage charging, or task-level energy delivery. Reporting these stages separately also makes it possible to distinguish successful electromagnetic coupling from successful energy transfer, which is essential when comparing harvesters with different source impedances or interface circuits. This paper does not report a harvested-power value because the available experimental dataset did not contain a reliable loaded-power measurement; the result is therefore an evaluation insight rather than a new quantitative power claim.

Second, the interface should be treated as part of the harvester design. More winding turns can raise induced voltage while also increasing winding resistance, and a passive bridge imposes forward-voltage loss and nonlinear loading before the PMIC sees any energy. The PMIC then adds its own input and startup constraints. These interactions mean that optimizing a pickup coil for voltage alone can be inconsistent with maximizing useful downstream energy. Coil, rectifier, and PMIC should instead be co-designed around the source impedance and expected operating load. In this view, the best front-end design is not necessarily the one with the largest lightly loaded voltage; it is the one that preserves sufficient voltage and current after connection to the interface so that downstream energy conversion can begin and remain stable.

Third, the final objective is energy delivered to storage or a load, not merely a visible induced voltage. In this prototype, the real harvesting chain stopped at the rectification stage, while the BQ25570 required an external approximately 3 V source for isolated testing. Low-forward-voltage rectification, lower winding resistance, impedance matching, buffering, and synchronous rectification are therefore reasonable future design implications, but none is presented as an experimentally verified improvement in this paper. The broader lesson is to evaluate powerline harvesters by the energy that survives the complete conversion chain.

6. Conclusion

This paper investigated why a powerline magnetic harvester can exhibit a substantial induced voltage without delivering usable downstream power. The front end was designed for approximately

DOI: 10.54254/2755-2721/2026.37436

6 V and produced 5.33 V AC at 10 A and 50 Hz, yet the bridge-rectifier output was 0 V DC and the real harvesting chain did not produce observable storage charging. A simplified source-impedance simulation qualitatively reproduced the progression from stable rectification for an ideal source to severe voltage collapse when source impedance and load were introduced. These results are consistent with a system-level mechanism in which source impedance, rectifier loss, and interface loading jointly limit energy transfer, although the actual source impedance was not directly measured. Powerline energy harvesting should therefore be designed and evaluated around loaded power delivery rather than induced voltage alone.

References

[1] Riba, J.-R., Moreno-Eguilaz, M., & Bogarra, S. (2022). Energy harvesting methods for transmission lines: A comprehensive review. *Applied Sciences, 12*(21), 10699. https://doi.org/10.3390/app122110699

[2] Wang, W., Huang, X., Tan, L., Guo, J., & Liu, H. (2016). Optimization design of an inductive energy harvesting device for wireless power supply system overhead high-voltage power lines. *Energies, 9*(4), 242. https://doi.org/10.3390/en9040242

[3] Yuan, S., Huang, Y., Zhou, J., Xu, Q., Song, C., & Thompson, P. (2015). Magnetic field energy harvesting under overhead power lines. *IEEE Transactions on Power Electronics, 30*(11), 6191–6202. https://doi.org/10.1109/TPEL.2015.2436702

[4] Martín Sánchez, P., Rodríguez Sánchez, F. J., & Santiso Gómez, E. (2020). An experimental strategy for characterizing inductive electromagnetic energy harvesters. *Sensors, 20*(3), 647. https://doi.org/10.3390/s20030647

[5] Zhuang, Y., Xu, C., Song, C., Chen, A., Lee, W., Huang, Y., & Zhou, J. (2020). Improving current transformer-based energy extraction from AC power lines by manipulating magnetic field. *IEEE Transactions on Industrial Electronics, 67*(11), 9471–9479. https://doi.org/10.1109/TIE.2019.2952795

[6] Park, B., Kim, D., Park, J., Kim, K., Koo, J., Park, H. H., & Ahn, S. (2018). Optimization design of toroidal core for magnetic energy harvesting near power line by considering saturation effect. *AIP Advances, 8*(5), 056728. https://doi.org/10.1063/1.5007772

[7] Moon, J., & Leeb, S. B. (2015). Analysis model for magnetic energy harvesters. *IEEE Transactions on Power Electronics, 30*(8), 4302–4311. https://doi.org/10.1109/TPEL.2014.2357448

[8] Monagle, D., Ponce, E., & Leeb, S. B. (2022). Generalized analysis method for magnetic energy harvesters. *IEEE Transactions on Power Electronics, 37*(12), 15764–15773. https://doi.org/10.1109/TPEL.2022.3195149

[9] Li, P., Wen, Y., Zhang, Z., & Pan, S. (2015). A high-efficiency management circuit using multiwinding upconversion current transformer for power-line energy harvesting. *IEEE Transactions on Industrial Electronics, 62*(10), 6327–6335. https://doi.org/10.1109/TIE.2015.2431648

[10] Cao, J., Jiao, Y., Meng, G., Peng, J., Stassi, S., Pirri, F., & Li, Y. (2022). A current transformer energy harvester with stable output based on the saturable magnetic core. *Electronics Letters, 58*(18), 705–707. https://doi.org/10.1049/ell2.12566

[11] Kabakulak, M., & Arslan, S. (2021). An electromagnetic energy harvester for wireless sensors from power lines: Modeling and experiment verification. *Gazi University Journal of Science, 34*(3), 786–806. https://doi.org/10.35378/gujs.764142

[12] Maharjan, P., Salauddin, M., Cho, H., & Park, J. Y. (2018). An indoor power line based magnetic field energy harvester for self-powered wireless sensors in smart home applications. *Applied Energy, 232*, 398–408. https://doi.org/10.1016/j.apenergy.2018.09.207

[13] Abramovitz, A., Shvartsas, M., & Kuperman, A. (2024). Design oriented analysis of overhead line magnetic energy harvesters with passive and active rectifiers. *Electronics, 13*(24), 4904. https://doi.org/10.3390/electronics13244904

[14] Texas Instruments. (2019, March). BQ25570 nano power boost charger and buck converter for energy harvester powered applications. *BQ25570 Datasheet*, Rev. G.